





An exploratory investigation of brain collateral circulation plasticity after cerebral ischemia in two experimental C57BL/6 mouse models

Marco Foddis^{1,*}, Katarzyna Winek^{1,*}, Kajetan Bentele², Susanne Mueller^{1,3}, Sonja Blumenau¹ , Nadine Reichhart N⁴, Sergio Crespo-Garcia⁴ , Dermot Harnett², Andranik Ivanov², Andreas Meisel¹, Antonia Jousen⁴, Olaf Strauss⁴, Dieter Beule², Ulrich Dirnagl^{1,5} and Celeste Sassi¹

Abstract

Brain collateral circulation is an essential compensatory mechanism in response to acute brain ischemia. To study the temporal evolution of brain macro and microcollateral recruitment and their reciprocal interactions in response to different ischemic conditions, we applied a combination of complementary techniques (T2-weighted magnetic resonance imaging [MRI], time of flight [TOF] angiography [MRA], cerebral blood flow [CBF] imaging and histology) in two different mouse models. Hypoperfusion was either induced by permanent bilateral common carotid artery stenosis (BCCAS) or 60-min transient unilateral middle cerebral artery occlusion (MCAO). In both models, collateralization is a very dynamic phenomenon with a global effect affecting both hemispheres. Patency of ipsilateral posterior communicating artery (PcomA) represents the main variable survival mechanism and the main determinant of stroke lesion volume and recovery in MCAO, whereas the promptness of external carotid artery retrograde flow recruitment together with PcomA patency, critically influence survival, brain ischemic lesion volume and retinopathy in BCCAS mice. Finally, different ischemic gradients shape microcollateral density and size.

Keywords

Stroke, collateral vessels, posterior communicating arteries, middle cerebral artery occlusion, bilateral common carotid artery stenosis

Received 5 September 2018; Revised 10 December 2018; Accepted 10 December 2018

Introduction

Collateral circulation represents an essential neuroprotective mechanism during severe acute brain ischemia–hypoxia. Despite the critical importance of collateral arteries, their clinical and neuroradiological assessment in patients remains a major challenge.^{1,2} First, collateral arteries represent a complex trait, highly influenced by genetic, sex and age-related variability. Second, they are recruited exclusively under moderate-severe acute ischemic conditions like transient ischemic attack (TIA) and strokes. Third, additional cardiovascular risk factors may frequently co-exist and exert an additive effect on the ischemia outcome (hypertension, diabetes, atherosclerosis, and aging). Finally,

¹Department of Experimental Neurology, Center for Stroke Research Berlin (CSB), Charité – Universitätsmedizin Berlin, Corporate Member of Freie Universität Berlin, Humboldt-Universität zu Berlin, and Berlin Institute of Health, Berlin, Germany

²Berlin Institute of Health, BIH, Unit Bioinformatics, Berlin, Germany

³Charité – Universitätsmedizin Berlin, NeuroCure Cluster of Excellence and Charité Core Facility 7T Experimental MRIs, Berlin, Germany

⁴Department of Ophthalmology, Experimental Ophthalmology, Charité Universitätsmedizin Berlin, Berlin, Germany

⁵QUEST Center for Transforming Biomedical Research, Berlin Institute of Health (BIH), Berlin, Germany

*These authors contributed equally to the work

Corresponding author:

Ulrich Dirnagl, Department of Experimental Neurology, Charité Universitätsmedizin Berlin, Berlin, Germany.
Email: Ulrich.Dirnagl@charite.de

standardized and validated neuroimaging methods to study collateral circulation are still lacking.^{1,2}

By contrast, inbred mice, minimizing genetic, epigenetic and environmental factors offer a unique window into the brain collateral circulation plasticity.^{3–5} Nevertheless, only few studies described collateral circulation in mice, mainly focusing on posterior communicating arteries (PcomAs) and leptomeningeal arteriole variability in different mouse strains.² Particularly, variability in the extension of the collateral circulation in terms of collateral number and diameter has been reported between C57BL/6 and BALB/cByJ mice that display high and low extent of collaterals, respectively, resulting in significantly different infarct volumes.⁶

On the other hand, intrasrain dynamic Pcoma patency and the hemodynamic response of the whole brain collateral circulation to compensate Pcoma variability remain largely unexplored.

This study aims to provide a comprehensive description of the macro and microcollateral artery plasticity during brain acute and subacute hypoperfusion in two experimental mouse models (MCAO and BCCAS). Therefore, we applied a combination of complementary techniques (T2-weighted magnetic resonance imaging [T2-MRI], arterial spin labeling cerebral blood flow [CBF], magneto resonance angiography [MRA] and histology) to study two C57BL/6J background brain hypoperfusion mouse models, where hypoperfusion is the result of either bilateral common carotid artery (CCA) stenosis (BCCAS) or 60-min unilateral blockage of the left middle cerebral artery (MCA) with permanent occlusion of CCA and external carotid artery (ECA) (MCAO).

Our study may provide potential insights that could be translated into the clinic, both in terms of a more informed use of these experimental models and better understanding of the brain collateral circulation.

Material and methods

Animals, experimental design and exclusion criteria

Experiments were approved by the Landesamt für Gesundheit und Soziales and conducted according to the German Animal Welfare Act and ARRIVE guidelines (<https://www.nc3rs.org.uk/arrive-guidelines>); 34 and 18 male C57BL/6J mice (purchased at 8 weeks of age, Charles River, Germany and 10 weeks of age Janvier France, respectively) were housed in a temperature ($22 \pm 2^\circ\text{C}$), humidity ($55 \pm 10\%$), and light (12/12-h light/dark cycle) controlled environment. The animals underwent hypoperfusion between 9 and 13 weeks of age ($n=42$, BCCAS = 27, MCAO = 15) or were used as controls (naïve = 7; MCAO sham = 3) (Figure S1(A) and (B))

The only exclusion criterion was death during MRI due to wrong placement of the animal in the scanner and led to exclusion of two MCAO and two sham animals (MCAO group), resulting in final analyzed sample size of MCAO = 13 and MCAO sham = 1.

BCCAS mice were imaged before surgery, 24 h and 1 week post-surgery. The BCCAS data from seven weeks are data from a previous study⁷ focused on the same BCCAS model. They are important to show that after seven weeks, the CBF recovery is associated to a complete circle of Willis (CoW) loop detected on MRA, analogously to the pre-surgery condition. MCAO mice were imaged 24 h, one week, four weeks and seven weeks post-surgery for angiography and estimation of CBF using arterial spin labeling. At two days and eight days (BCCAS) and seven weeks (MCAO), tissue was processed for immunohistochemistry

Histology

PFA perfused brains were cut into 50- μm -thick sections on a cryostat. After washing with phosphate-buffered saline (PBS), free-floating sections were incubated with 10% normal goat serum (NGS, GeneTech, GTX27481) and 0.1% Triton-X-100 (Sigma-Aldrich, X100) in PBS for 1 h at room temperature to block unspecific binding. Primary and secondary antibodies were diluted in 1% NGS and 0.1% Triton-X-100 in PBS. Sections were incubated with rat anti-GFAP primary antibody (Millipore, 345860) for astrocytes and rabbit anti-Iba-1 primary antibody (Wako Chemicals, catalog #019-19741; RRID: AB_839504) for microglia and macrophages at 4°C overnight. After thorough washing, sections were incubated at room temperature with AlexaFluor-594-conjugated goat anti-rat (Invitrogen, catalog #A11081) and AlexaFluor-488-conjugated goat anti-rabbit (Invitrogen, catalog #A11034) secondary antibodies for 2 h at room temperature. Wheat Germ Agglutinin (WGA) Alexa Fluor 680 conjugate anti-lectin together with Evans Blue was used to stain blood vessels (further details in supplemental materials and methods). Nuclei were counterstained with DAPI (Fluka, 32670). Sections were mounted with anti-fading mounting medium Shandon Immuno Mount (Thermo Scientific, 9990402) on Super Frost Plus glass slides (R.Langensbrinck, 03-0060). Microphotographs were taken with a confocal microscope (Leica TCS SPE; RRID: SciRes_000154).

Methods to prevent bias, statistics

This is an exploratory, descriptive study. Sample sizes were not based on *a priori* power calculation. Only

descriptive but no test statistic was used. Mice were randomized to receive hypoperfusion.

PcomA size

Following Martin et al.,⁸ we grade the PcomA patency in hypoperfused mice, using the ratio between PcomA and basilar artery (BA) diameters. Martin and colleagues identified four PcomA classes in naïve mice: (1) PcomA <10% of BA; (2) PcomA 11–20% of BA; (3) PcomA 21–30% of BA and (4) PcomA >30% of BA. Although we are convinced that PcomA patency is a functional phenotype that can only be observed after PcomA recruitment, we kept the same classification for hypoperfused mice, where both PcomA and BA diameter are increased, leaving, to different extents, the PcomA/BA ratio likely similar to the one observed in naïve mice. Based on our experiments, class 1 and class 2 have been detected either in naïve mice or MCAO and BCCAS mice that died few hours post-surgery, strongly arguing for a non-patent PcomA. Therefore, we identify class 1 and class 2 as ‘non-patent’, class 3 as ‘small’, class 4 as ‘prominent’ and introduce a fifth class, represented by PcomA>60% of BA, described as ‘very prominent’.

The diameters of the PcomAs were measured at the smallest point and the diameter of the BA was measured proximal to the superior cerebellar arteries both for the Evans Blue and fluorescent WGA stainings with ImageJ. The diameter of the PcomAs as a percentage of the diameter of the BA was calculated and used in the analysis as previously described⁸ (Figure S2(A) and (B)).

Angiotool

Vascular density, vessel length, end points, total vascular junctions and junction density were calculated for both striatal, cortical and leptomeningeal microvessels, selecting always the same regions of interest (both in terms of brain area in both hemispheres and region of interest dimension) by using the software *AngioTool* v0.6a as previously described (Figure S2(C) and (D)).⁹

Additional information is included in the supplementary materials.

Results

Macrocollaterals (PcomAs, AcomA and ECA branches) in BCCAS and MCAO mice

In this study, we used two inbred hypoperfusion mouse models (BCCAS and MCAO) (Figure S1(A) and (B)) with C57BL/6J background to describe and analyse collateral artery plasticity in response to acute and chronic brain hypoperfusion.

We show that in naïve mice PcomAs are very small and not identifiable on MRA, basilar artery and posterior cerebral arteries, affluents and effluents of PcomAs, respectively, are subtle (Figure 1(A), Figure S3(A)). By contrast, in presence of an acute focal ischemia, PcomAs become prominent vessels up to $\approx 60\%$ of the basilar artery diameter. Their recruitment in the first hours post-surgery is essential for the mouse survival and CBF sustainment and is characterized by an increasingly intense MRA signal (Figures 1(C) and (D) and 2(A) to (C); Figure S3(B) to (D)). These MRA findings have been confirmed with anatomical ones (Evans Blue and WGA CoW stainings in naïve, BCCAS and MCAO mice) (Figures 1(A) to (D) and 3(G) and (M); Figures S2(A) and (B) and Figure S3).

Among the nodes of the collateral artery circuit (anterior communicating artery [AcomA], PcomAs, ECA, ophthalmic artery and leptomeningeal vessels and other deep microcollaterals), PcomAs display a different degree of patency, critically influencing the ischemic lesion volume, resolution and overall CBF recovery. The atresia of the PcomA ipsilateral to the MCAO and the hypoplasia of one PcomA together with the late recruitment of ipsilateral external carotid artery retrograde flow in BCCAS are likely responsible for lethal strokes affecting up to 34% of one hemisphere (12/27 [44.4%] and 3/13 [23%] BCCAS and MCAO mice, respectively) (Figure 1(E) to (J)).

On the other hand, the presence of small to very prominent PcomAs (15/27 [55.5%] and 10/13 [77%] BCCAS and MCAO mice, respectively) guaranteed the survival during the most severe hypoperfusion (one day post-surgery, $\approx 70\text{--}80\%$ CBF drop) (Figure 1(E) and (F); Figure S3(B) to (D)).

Moreover, in a minority of mice, the collateral recruitment was particularly rapid and effective, leading to no lesions (defined as white or gray matter hyperintensities) detectable on T2 MRI during the first week post-surgery (BCCAS 2/27 [7.4%], at least one prominent PcomA together with bilateral recruitment of ECA retrograde flow one day post-surgery) (Figure 2(F); Table S1) or small lesions (1–5% of the left hemisphere) confined to striatum and dorsal part of the prefrontal cortex (MCAO, 7/13 [53.8%], prominent/very prominent left PcomA) (Figure 3(A) and (O)).

BCCAS (30% stenosis of both CCAs: Left CCA stenosis [surgery day 1], right CCA stenosis [surgery day 2])

BCCAS is the result of a two-day surgery beginning first with a left CCA stenosis of approximately 30% and after one day with the stenosis of the right CCA (Figure S1(A)). The compensatory mechanisms activated at day 1 deeply affect also day 2 outcome.

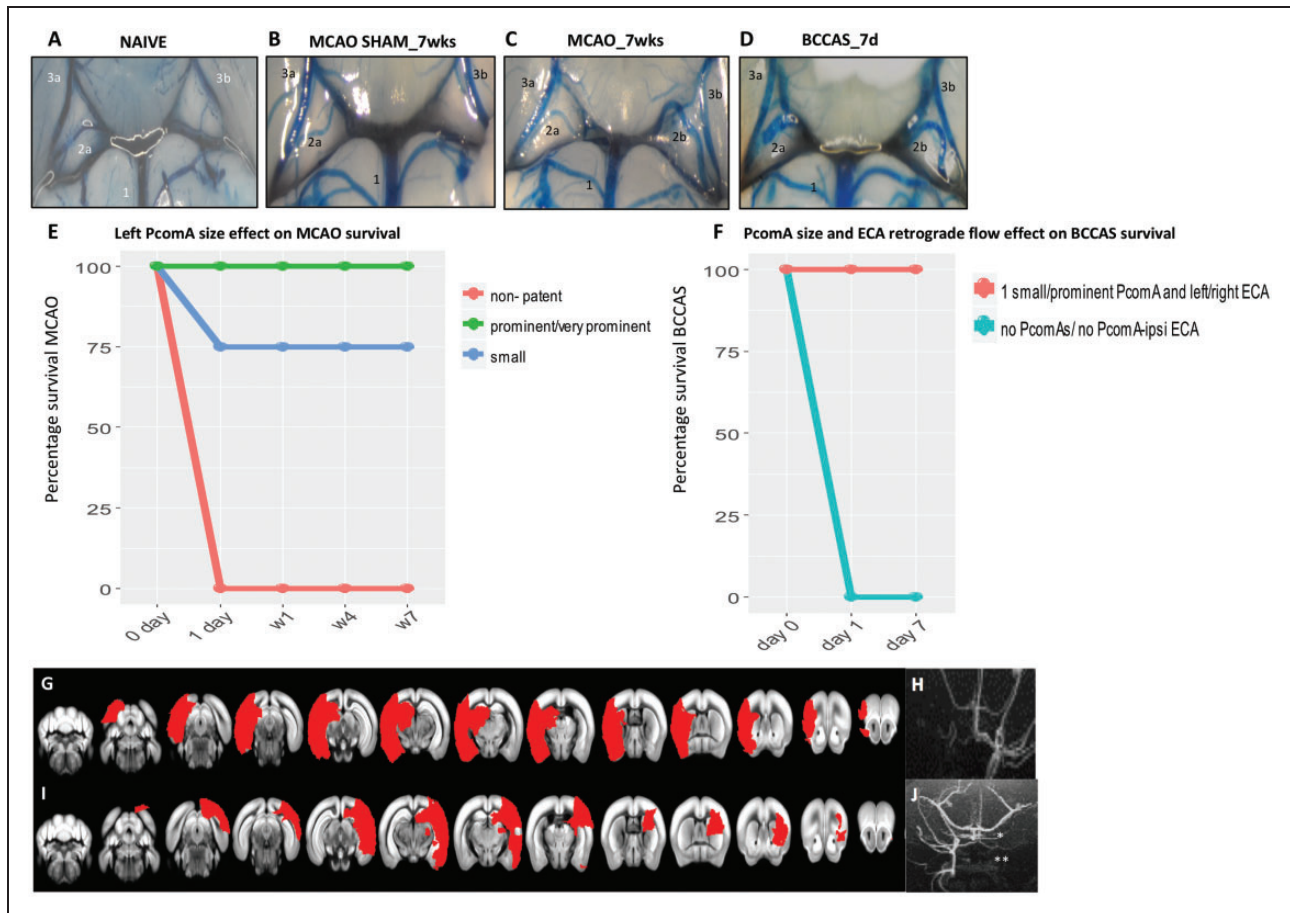


Figure 1. PcomA and vascular phenotype effect in MCAO and BCCAS mouse models. (A–D). PcomA calibre in normal and ischemic conditions. (A) Non-patent right PcomA (2a), detected in a naïve mouse; (B) non-patent right PcomA (2a) and absence of left PcomA in MCAO sham; (C) prominent left PcomA (2b) and non-patent right PcomA (2a) in MCAO; (D) 2 prominent PcomAs in BCCAS (2a, 2b). 1, basilar artery (BA); 2a, right PcomA; 2b, left PcomA; 3a, right posterior cerebral artery (PCA); 3b, left posterior cerebral artery (PCA). The numbering of the vessels reflects the direction of the collateral blood flow following focal ischemia in the MCA or anterior brain areas: BA→PcomA→PCA, as already described in detail in the BCCAS and MCAO models in Figure S1 (A) and (B). (E–F) Effect of left PcomA size and PcomA-ECA retrograde flow in MCAO and BCCAS survival. MCAO mice with non-patent left PcomA die few hours post-surgery. ≈ One-fourth of mice with small left PcomA die within one day post-surgery. The majority of MCAO mice with small left PcomA and all the MCAO with prominent/very prominent PcomA survive (E). Analogously, BCCAS mice with no PcomAs or no PcomA-no ipsilateral ECA retrograde flow die within few hours post-surgery. By contrast, BCCAS mice with at least one small to prominent PcomA and retrograde flow from left or right ECA do survive (F). (G–H) MCAO mice with non-patent left PcomA died within one day post-surgery with ischemic lesions affecting more than 35% of the left hemisphere and left PcomA and overall left blood flow were not identifiable on MRA one day post-surgery. (I–J) BCCAS with non-patent right PcomA (*) and absence of right ECA retrograde flow recruitment (**), presenting severe ischemic lesions affecting >20% of the right hemisphere.

The CBF reduction in the left hemisphere one day post-surgery reaches an average of 72% (20%–98%) in left striatum and frontal cortex (Figure 2(G); Tables S2 and S3). This severe CBF drop likely instantly recruits (a) left PcomA, (b) AcomA and (c) left ECA retrograde flow (Figure 2(A) and (B)). The AcomA likely redistributes blood flow from the right to the left hemisphere, with an overall reduction of right CBF and a consequent increased vulnerability for ischemic lesions during the surgery on this remaining side. Indeed, one day post-surgery, arterial border zones between right anterior

cerebral artery (ACA) and right MCA were the most susceptible areas (Figure 2(Ba); Figures S4 and S5).

A total of 20 out of 27 mice (74%) presented small to moderate ventral subcortical lesions affecting overall 1%–37% of the right hemisphere, and particularly right striatum (17/20 [85%]), prefrontal cortex (14/20 [70%]), hippocampus (10/20 [50%]) and corpus callosum (5/20 [25%]) (Figure 2(H); Table S4). These lesions were associated with a right CBF reduction which was more severe (82% [range: 60%–95%]), compared to the one observed in the left side (Figure 2(G); Tables S2

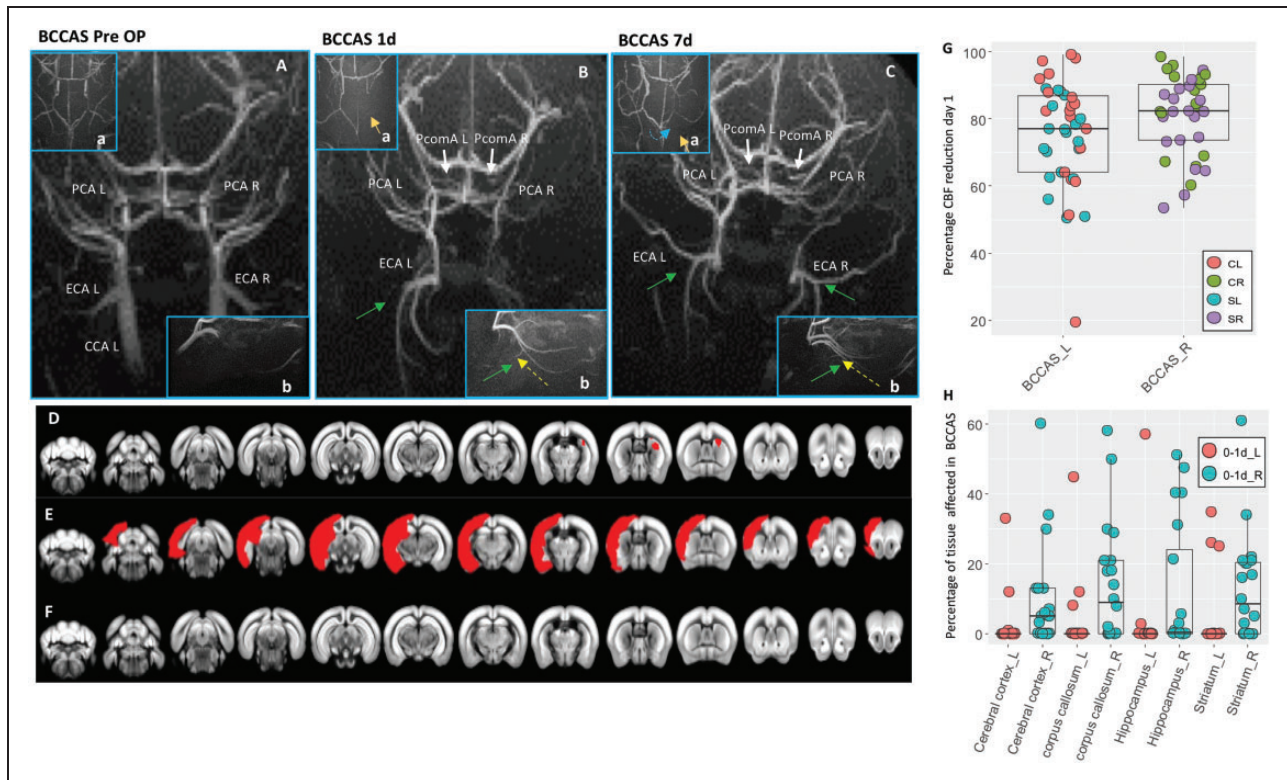


Figure 2. MRA and MRI phenotypes in BCCAS mice one to seven days post-surgery. (A–C) Vascular collateral plasticity during the first week post-surgery; (a), circle of Willis; (b), ECA flow. (A) Pre-surgery MRA, where PcomAs are not identifiable. (B) MRA one day post-surgery, showing recruitment of both PcomAs (white arrows), directing the blood flow to the PCAs, whose MRA intensity is increased, and left ECA retrograde flow (green arrow, yellow dashed line) and hypoperfused border zones between right ACA and right MCA (a, orange arrow). (C) MRA seven days post-surgery, characterized by increased PcomA (white arrows) and PCAs MRA intensity signal, recruitment of right ECA retrograde flow (green arrow, yellow dashed line), with a compensatory sustainment of the right anterior cerebral artery (ACA) territory (a, orange arrow) partially coming from the left hemisphere through the AcomA (blue dashed line). (D–F) Main ischemic lesion patterns observed in BCCAS 24 h post-surgery on T2-weighted MRI: small right subcortical lesions (D), big cortical and subcortical lesions (E) and no lesions detectable (F). (G) Percentage of CBF reduction at day 1 in BCCAS mice in left and right hemispheres, displaying more accentuated hypoperfusion in the right hemisphere, particularly in the frontal cortex. (H) Most affected brain regions in the BCCAS model 1 day post surgery are the watershed areas between right ACA and right MCA: right cerebral cortex, corpus callosum, striatum und hippocampus. CCA L: left common carotid artery; ECA L: left external carotid artery; ECA R: right external carotid artery; PCA L: left posterior cerebral artery; PCA R: right posterior cerebral artery; PcomA L: left posterior communicating artery; PcomA R: right posterior communicating artery. R: right; L: left. Pre-Op, pre-surgery.

and S3) and to the absence of retrograde flow from right ECA, which, on the contrary, was already present in the left side (Figure 2(A) and (B)).

Recruitment of retrograde flow from ECA and PcomA patency are the main factors influencing CBF and therefore lesion extension and overall recovery (Figures 1(F) and (J) and 2; Figure S5). However, the significant intra-strain variability of PcomAs and ECA retrograde flow recruitment leads to markedly different degrees of hypoperfusion. Among the mice with at least one patent PcomA, surviving during the first week post-surgery (15/27 [55.5%]), we identified three main neuroimaging and vascular phenotypes: (1) mice presenting small subcortical lesions, generally affecting right watershed areas (5%–20% of the right striatum and corpus

callosum, 10/15 [66.6%]), displaying at least one prominent and one small PcomAs and retrograde flow from left ECA at day 1 (Figure 2(A) to (D); Figure S5(A); TableS1); (2) mice presenting different degrees of ischemic lesions in the left hemisphere (3/15 [20%]), associated to absence of retrograde flow from left ECA and one prominent PcomA (Figure 2(E); Figure S5(B); TableS1) and (3) mice with no ischemic lesions both at one day and seven days post-surgery (2/15 [13.3%]), displaying at least one prominent PcomA and retrograde flow from both ECAs (Figure 2(F); Figure S5(C); TableS1). Importantly, even if the CBF drop may not cause ischemic lesions detectable on T2 MRI, mild hypoperfusion leads to migration and activation of microglia/macrophages and astrocytes (Figure S6).

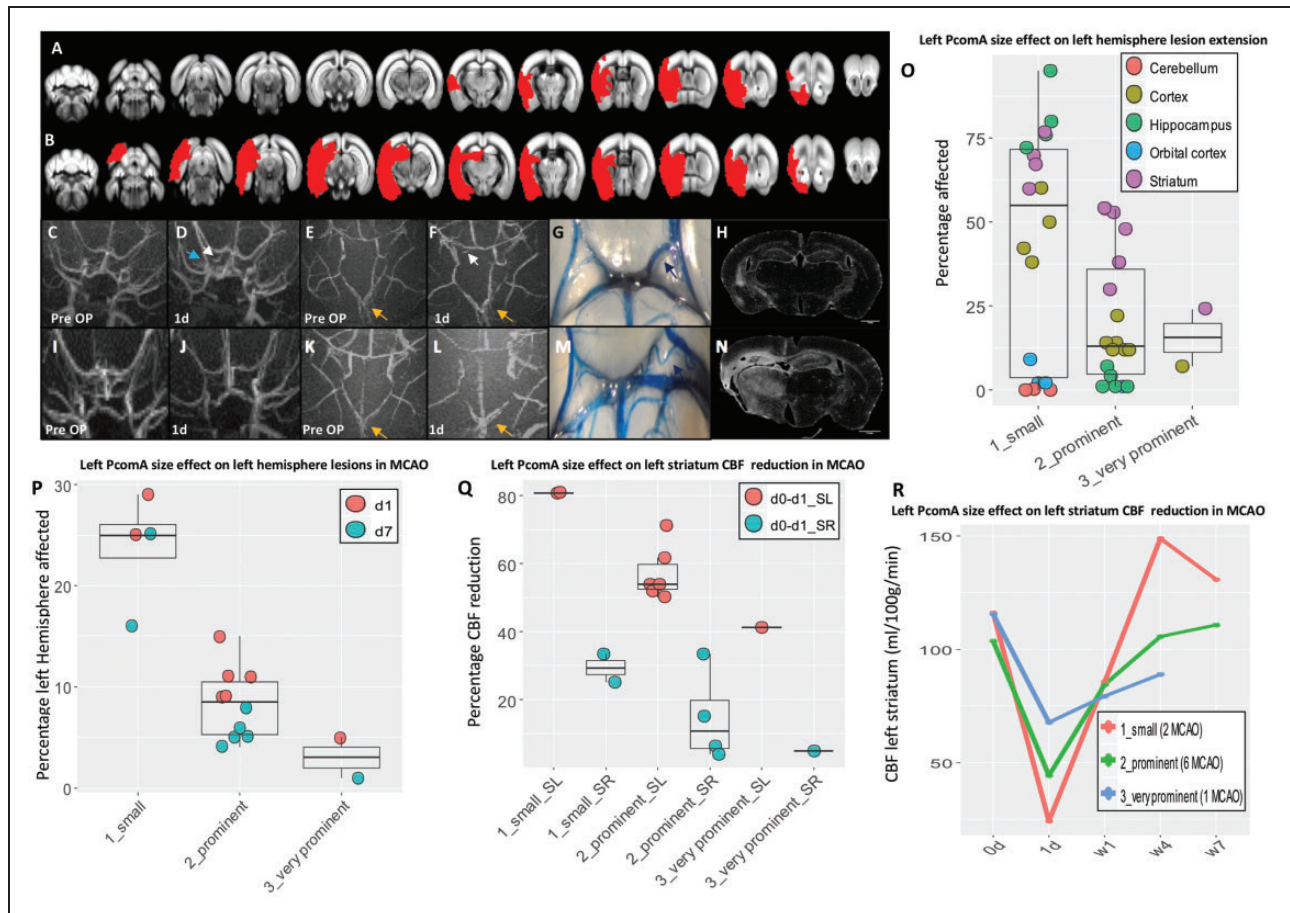


Figure 3. Effect of PcomA in MCAO. (A–B) ischemic lesions (red shades) identified on T2-weighted MRI. (A–N) Edges of the phenotypic spectrum observed in MCAO mice: small lesion (A) associated to very prominent left PcomA (C–G) and absence of macroscopic left atrophy (H). (C–D) Recruitment of left PcomA is identifiable on MRA one day post-surgery (white arrow) and it is accompanied by increased intensity of left PCA (blue arrow). (B) Extensive lesion caused by small left PcomA (I–M), leading to significant left brain atrophy (N). (E–F) and (K–L) progressive increase in the Acoma size (yellow arrows). (O–R) PcomA size is the most important factor in determining lesion volume during acute hypoperfusion (one day), infarct resolution during subacute hypoperfusion (seven days) (O, P, Q), ipsilateral and compensatory contralateral CBF decay in ventral ischemic regions such as striatum (Q, R). Detailed description of MCAO mice phenotype as well as collateral blood flow direction is provided in the supplementary materials. Small, prominent and very prominent refer to the left PcomA size. SL: striatum left; SR: striatum right; d: day/s; w: weeks.

External–internal carotid shunt via ophthalmic artery in BCCAS mice

Although we could not assess the ophthalmic artery flow using a Doppler ultrasonography, we have used angiography and histology to study the retina. Seven days post-surgery, we report severe retina degeneration with gliosis particularly in the ganglion cell layer and moderate loss of presynaptic protein CTBP2 in the outer plexiform layer. During chronic hypoperfusion, we observe severe thinning and retinal atrophy mostly in the ganglion cell layer and inner nuclear layer, with significant reduction of CTBP2 signal (Figure S7(A) to (C)). Despite the recruitment of ancillary branches of the

ECA and a likely external-internal shunt, as already reported in patients with internal carotid occlusive disease,^{10,11} we show that retinal degeneration is irreversible. This is likely due to either the late recruitment of retrograde flow through the ECA or the pre-existence of external-internal carotid shunt (retrograde flow from the eye to the brain) via ophthalmic artery or both with an overall reduction of blood flow to the retina.

MCAO (left MCA, CCA and ECA occlusion)

MCAO is the result of surgery consisting of 60-min transient blockage of left MCA and permanent occlusion of CCA and ECA (all in one session) (Figure

S1(B)). This causes a significant drop in CBF in the ipsilateral hemisphere. One day post-surgery, the average CBF reduction is $\approx 60\%$ (range: 22%–81%) in ipsilateral striatum and frontal cortex (Tables S5 and S6). This acute and severe hypoperfusion, likely causes a hemodynamic gradient between anterior hypoperfused brain areas and posterior areas normally perfused. The blood flow in left PcomA and the more intense AcomA signal, detected one day post-surgery on MRA, is an indirect indication of left PcomA and AcomA patency (Figure 3(C) to (F), (K) and (L)). A new global and stable hemodynamic balance close to the baseline is reached in 9/10 (90%) mice seven days post-surgery (Table S5) and left PcomA and AcomA from ancillary vessels became critical vessels (Figure 3(D) to (G) and (K) to (L); Figure S8(A)).

Despite this general pattern, high intra-strain variability of PcomA patency is the most important factor in determining the stroke outcome. Indeed, it significantly influences the lesion volume, the lesion extension, the CBF recovery and the contralateral drop in CBF (Figure 3(O) to (R); Tables S6 and S7). In our cohort, we report a spectrum of left PcomA sizes, from non-patent and small (Figure 3(M), 4/13 [30.7%] and 2/13 [15.4%], respectively) to prominent and very prominent (Figure 3(G), 6/13 [46%] and 1/13 [7.7%], respectively). Mice with left non-patent PcomA died within few hours post-surgery. MCAO mice with a small left PcomA (Figure 3(M); S8(B)) displayed the largest lesions affecting up to 34% of the left hemisphere (Figure 3(B)) and including also dorsal areas (orbital cortex and cerebellum) (Figure 3(B), (O) and (P); Table S8), the most severe drop in CBF (up to 80% in left striatum) (Figure 3(Q) and (R)), the slowest recovery (up to four weeks) (Table S5) and a marked brain atrophy (Figure 3(N)). In these mice, we observed a significant proportional compensatory decrease of contralateral CBF (up to 30% in right striatum, Figure 3(Q)). In comparison, mice with prominent left PcomA (Figure S8(A)) showed lesions 2.6 times smaller (Figure 3(P); Table S7), mostly affecting ventral areas (prefrontal cortex, striatum and ventral hippocampus) (Figure 3(O)) and a moderate drop in ipsilateral and contralateral CBF ($\approx 57\%$ and 15% in left and right striatum, respectively) (Figure 3(Q)). Very prominent PcomA (Figure 3(G)) was associated to the smallest lesions (5% of the left hemisphere) (Figure 3(A)), mild CBF reduction, more rapid recovery (Figure 3(Q) and (R)) and absence of macroscopic ipsilateral brain atrophy (Figure 3(H)).

In the supplementary, we describe in details the extreme phenotypes. The other cases fall within this phenotypic spectrum (Figure S8).

The hemisphere contralateral to MCAO

In MCAO mice, the blood flow redistribution from the right to the left hemisphere via AcomA causes a significant and proportional CBF reduction in the right hemisphere: 17% (range: 4%–33%), 28% (range: 18–41%) in striatum and frontal cortex, respectively (Figure 3(Q); Tables S5 and S6). Interestingly, MCAO mice with small left PcomA display significantly lower global CBF values, both for the left and right hemisphere at day 1 (Figure 3(Q); Tables S5 and S6) and right CBF reduction ($\approx 30\%$ in right striatum) which is close to the CBF reduction seen in BCCAS mice with the most effective vascular phenotype (retrograde flow from both ECAs and two prominent PcomAs) ($\approx 40\%$) at day 7 (Tables S3 and S6). This pattern mimics the hemodynamic effects of unilateral CCA stenosis and therefore triggers analogous compensatory mechanisms such as right ECA retrograde flow, although temporarily and only during the first 24 h post-surgery (Figure S8(C)). On the contrary, a more stable involvement of the contralateral hemisphere is evident at the microvascular level (leptomeningeal arterioles and deep microvessels), where increased number of larger arterioles and a more dense vascular network are detected in the infarct and peri-infarct areas, respectively, seven weeks post-surgery (Figures 4 to 6).

Microcollaterals (leptomeningeal and deep arterioles) in BCCAS and MCAO mice

In both models, part of the microvessels likely represent microcollaterals, given the increased number of vessel length, vascular junctions and reduction of end points compared to naïve mice (Figure 5(E) to (G)). These microvessels display in the cortical and deep gray matter a similar pattern, whereas the white matter arterioles appear significantly rare and sparse (Figures 4 and 5; Figures S9 and S10)

Infarct and peri-infarct areas and other hypoxic regions are characterized by significantly different microvascular features. Increased size up to 50 μm diameter and reduced density of arterioles are a hallmark in the infarct area (Figure 4(A) to (CIV); Table S9). Their increased diameter is associated with a significant invasion of microglia/macrophages, generally in the form of islets (Figure 4(CI) and (CII)) during the hypoxic subacute phase, whereas activated astrocytes are detected in the peri-infarct area and delimit the infarct-peri-infarct border (Figure 4 (CIII)). By contrast, the peri-infarct area and moderately hypoperfused regions are characterized by a network of microvessels with moderately increased length and whose number of anastomoses is proportional to the degree of hypoperfusion (highest density of junctions

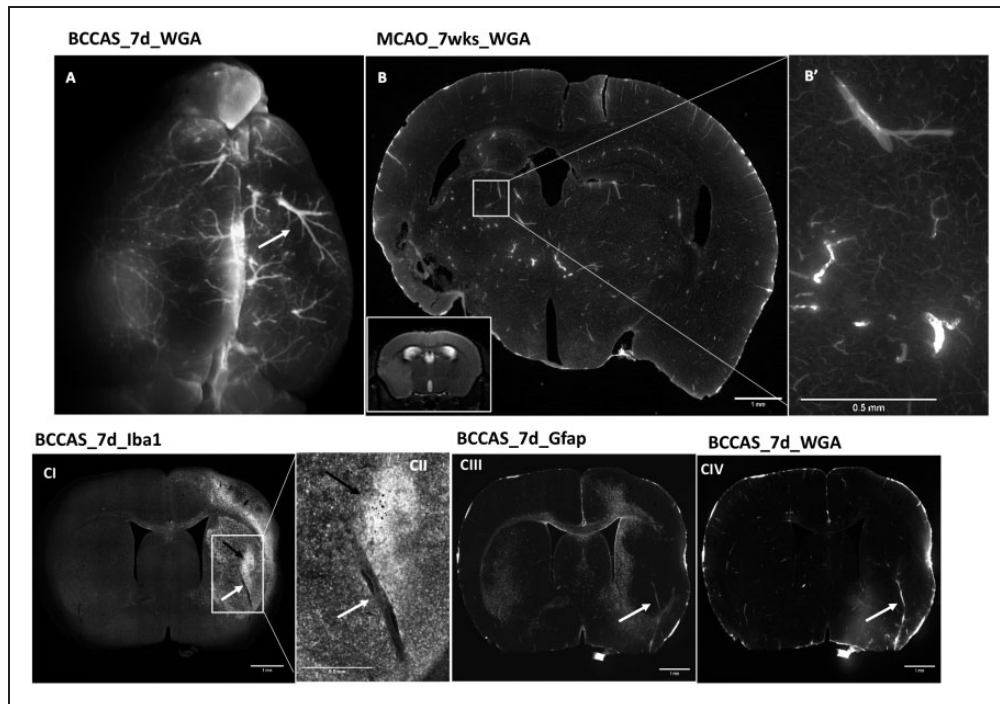


Figure 4. Microvascular plasticity in the infarct area in MCAO and BCCAS models. The infarct area is characterized by arterioles reduced in number and increased in size both at the leptomeningeal level (A) and striatal one (B–CIV)(white arrows), generally associated in the subacute phase (seven days) to significant microglia infiltration (CI–CII). Scale bars: B, CI, CIII, CIV = 1 mm; B', CII = 0.5 mm. Mice perfused with WGA Alexa Fluor® 680 conjugate (Thermofisher, W32465). D: day/s; wk: weeks.

in right and left hemisphere in BCCAS and MCAO mice, respectively) (Figure 5(E); Table S10). Importantly, in MCAO, this phenomenon affects also the relatively hypoperfused hemisphere contralateral to the focal ischemia and at the leptomeningeal superficial level gives rise to a symmetric picture, with both right and left leptomeningeal vessels presenting overlapping vascular anastomoses, vessel density and length seven weeks post-surgery (Figure 6(C) to (F); TableS11).

Discussion

The aim of the study was to capture the collateral vessel evolution during brain ischemia and to comprehensively describe the hemodynamic changes over time (one day, seven days, four and seven weeks) in two widely used experimental models of brain hypoperfusion with C57BL/6J background: MCAO and BCCAS.

We show that contralateral hemisphere, vertebrobasilar circulation and retrograde flow from ECA represent three essential reservoirs for the CBF redistribution during focal ischemia. In presence of acute ischemia, these three pools, normally independent, are interconnected by AcomA, PcomAs and ECA ancillary branches and become a pivotal and integrant part of the same hemodynamic circuit. Moreover, the

partial functional overlap between them leaves the possibility for some backup solutions.

PcomAs are the main determinants of stroke survival in MCAO. First, MCAO mice with no/non-patent PcomAs die within 24 h post-surgery. Second, MCAO mice display lesion volume, lesion resolution and ipsi and contralateral CBF reduction proportional to the left PcomA calibre, with mice with small and very prominent PcomAs showing the biggest and smallest lesion volumes and least and most effective lesion resolution, respectively (Figure 3). Analogously, PcomA patency together with the promptness of ECA retrograde flow recruitment plays a key role in BCCAS.

Overall, in both these hypoperfusion mouse models, we report a similar percentage of PcomA variability with 15.4% and 37% mice with none or two non-patent PcomAs, 30.8% and 22.2% mice with at least one small PcomA, 53.8% and 37% with one prominent/very prominent PcomA and 33.3% mice with two prominent PcomAs. By contrast, McColl et al.³ reported in the same C57BL/6 strain 3/10 (30%), 6/10 (60%) and 1/10 (10%) mice with none, one and two PcomAs, respectively.³ This difference may be due to three main factors: first, McColl studied the collateral status in naïve mice and we show that collaterals are recruited under moderate-severe acute hypoxia, therefore representing a functional vascular phenotype that

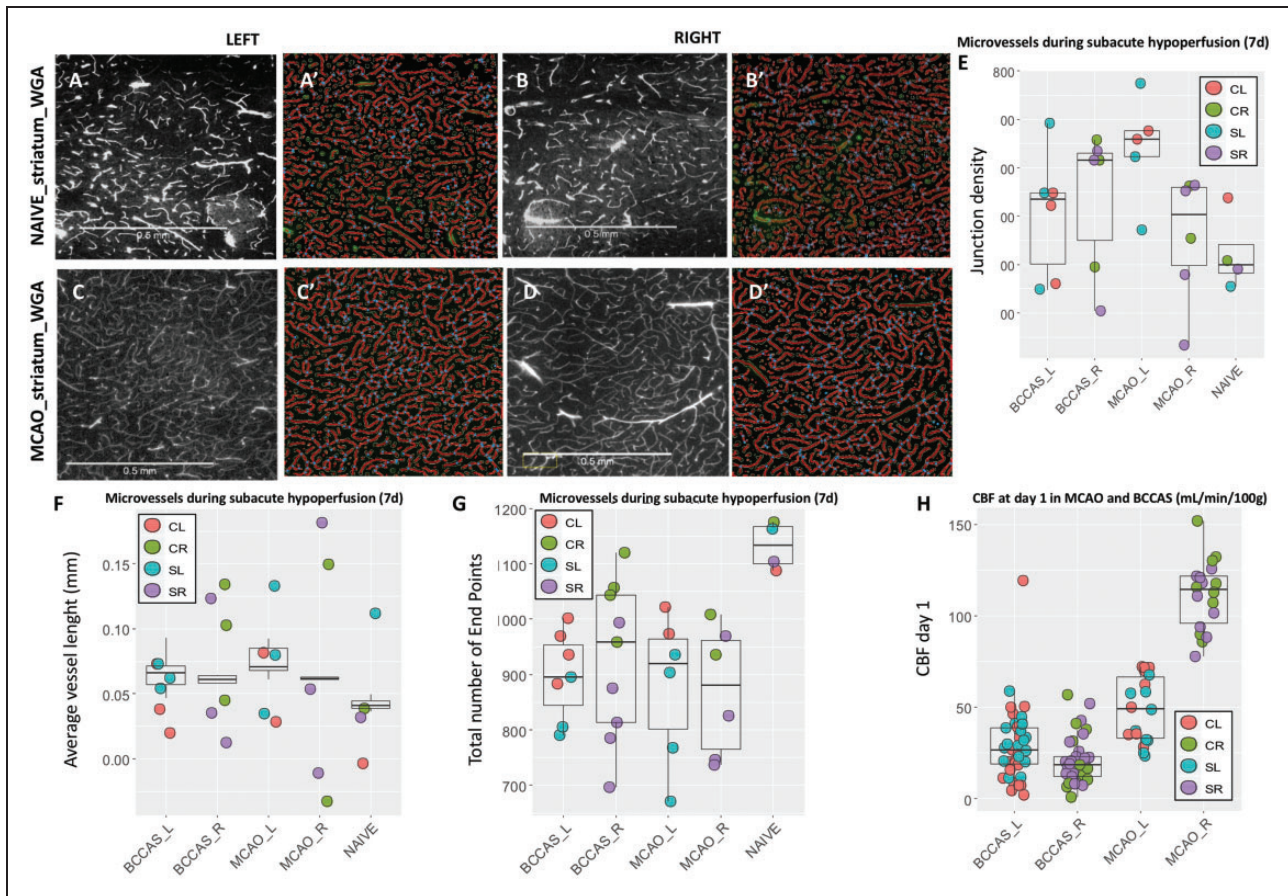


Figure 5. Moderately hypoperfused areas are characterized by microvessels with moderately increased length in MCAO compared to naïve mice (A–D', F), whose significantly increased number of anastomoses (E–G) is proportional to the degree of hypoperfusion at day 1 (H). (A–B' and C–D') Microvessels stained with WGA in left and right striatum in naïve and MCAO mice, respectively. (A'–B' and C'–D') angiotool analysis of the homologous histological sections (A–B and C–D). Mice perfused with WGA. Scale bars = 0.5 mm. Alexa Fluor® 680 conjugate (Termofisher, W32465). L: left; R: right; CL: cortex left; CR: cortex right; SL: striatum left; SR: striatum right.

can only be seen in response to ischemia. Thus, the presence of very subtle vessels in naïve mice does not imply their potential patency. Second, the small sample size that can significantly bias the results. Third, PcomA size represents a dynamic spectrum, varying significantly from non-patent to very prominent and therefore an unambiguous classification is difficult to draw.

A growing body of evidence reported hemodynamic, metabolic, neuroimaging and functional changes in the stroke contralateral hemisphere in the acute phase (first hours-days post ischemia).^{12–16} Here, we provide evidence that the contralateral hemisphere represents an important reserve of blood flow that can be shifted to the ischemic focus, to counterbalance any CBF gradient. First, the average reduction of right CBF in the BCCAS model ($\approx 83\%$) is higher compared to the hypoperfusion detected in left hemisphere ($\approx 72\%$), likely due to the pre-existent right to left CBF shunt

due to the surgery on left CCA at day 1, the left-right CBF gradient drop and the later recruitment of the right ECA. Consequently, the right ACA territory and the border zones between right MCA and right ACA become particularly susceptible to ischemic lesions (Figure 2 (Ba); Figures S4 and S5). Second, MCAO right CBF reduction is proportional to the reduction of CBF in the left hemisphere and thus to the left PcomA calibre (Figure 3(Q); Table S6). This is in line with previous studies in patients that measured CBF with positron emission tomography (PET) and found a significant correlation between flow impairment in the ischemic area and proportional CBF reduction in the contralateral hemisphere.¹² Third, the CBF drop in MCAO mice with small left Pcoma (up to 37% of the pre-surgery value) is very close to the CBF reduction seen in BCCAS mice with two prominent PcomAs and retrograde flow from both ECAs seven days post-surgery ($\approx 40\%$) (Tables S3 and S6). Therefore, this

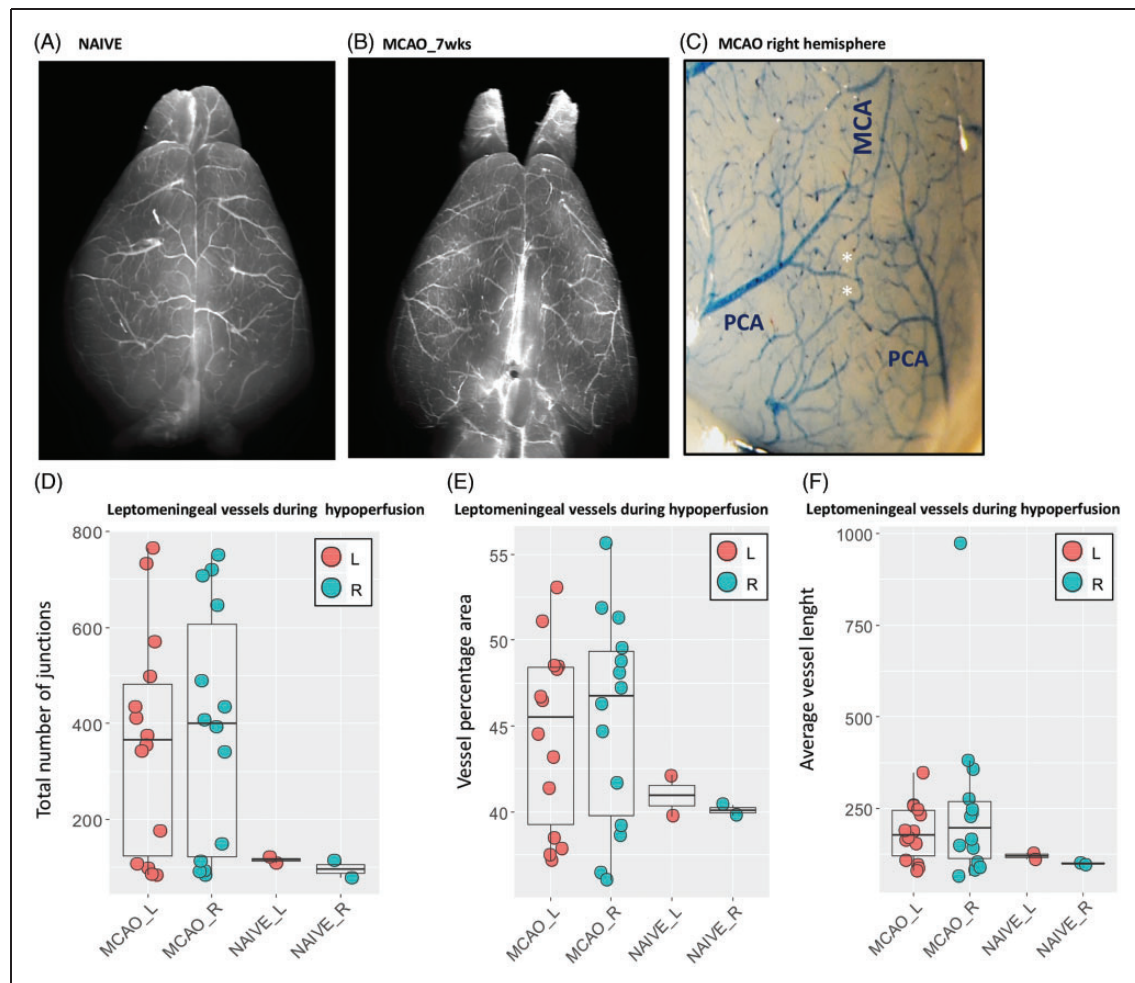


Figure 6. (A–F) Leptomeningeal vessels in MCAO mice seven weeks post-surgery. Leptomeningeal vessels in naïve mouse (A) and MCAO (B). (C) Anastomoses between terminal branches of PCA and MCA in the right cortex of MCAO mice. MCAO mice are characterized by a symmetric network of leptomeningeal arterioles with increased anastomoses (D), density (E) and moderately increased vessel length (F), both in cortex ipsilateral and contralateral to MCAO. MCA: middle cerebral artery; PCA: posterior cerebral artery; L: left; R: right; wks: weeks.

simulates the hemodynamic effects of a CCA stenosis and thus temporarily triggers the same compensatory mechanisms such as right ECA retrograde flow (Figure S8(C)). Moreover, the critical importance of the contralateral hemisphere in the sustenance of the CBF is highlighted by the different time of recovery between MCAO mice and BCCAS; 90% of MCAO mice recover almost to the baseline after one week, whereas BCCAS mice take four weeks.⁷ Finally, the significant involvement of the contralateral hemisphere leads to a moderate hypoperfusion that even if it is not sufficient to cause ischemic lesions and remains below the threshold of T2-weighted MRI detectability, is responsible for a significant microvascular remodelling at different levels: from the superficial leptomeningeal to the deep striatal layers (Figures 5 and 6).

Analogously to the peri-infarct area, moderately hypoxic ipsilateral and contralateral areas are covered with a dense network of microvessels with moderately increased length and significantly augmented anastomoses (Figure 5). Given its hemodynamic features, this microvascular phenotype likely results in a greater perfusion volume thus improving the tissue oxygenation and the uptake of catabolites. Moreover, this vascular web likely exerts a trophic function through the synthesis and release of neurotrophins such as NGF, IGF-I, and BDNF, that further catalyse the long-lasting vessel formation and recruitment of immune cells.¹⁷ Therefore, this hypoxia-triggered-vascular plasticity may shape and significantly influence pre-existent neuronal circuits, explaining neurophysiologic changes also in the contralateral hemisphere.¹⁸

By contrast, and as already reported in stroke patients,¹⁹ the infarct area is characterized by rarefied arterioles with increased diameter, up to 4.5 times the diameter of the largest arterioles observed in the respective brain regions in naïve mice (Figure 4; TableS9). These vascular features assure a reduced resistance and are particularly effective for a rapid delivery of microglia/macrophages, removing debris and exerting a neuroprotective function in the subacute phases (seven days post-surgery) (Figure 4(CI) and (CII)).^{20,21}

In addition, the abrupt redistribution of blood in ancillary vessels or vessel normally characterized by lower intravascular pressure causes macromodifications such as increased tortuosity, which is a hallmark of intravascular hypertension (Figure 3(M), blue arrow; Figure S8(A) and (B)).^{22,23} Over time, this may lead to (1) arteriolar hyaline in microvessels,²⁴ with an increased risk for subcortical microbleeds, already reported in the same BCCAS model, six months post-surgery⁷ and differing from amyloid related microbleeds, given the main subcortical location and the absence of lobar involvement²⁵ and (2) aneurysms in macrovessels.^{22,23} Therefore, strengthening a possible cause-effect link between ischemic and haemorrhagic strokes, which is supported already by several genetic risk factors such as *COL4A1* associated to both.^{26,27}

Finally, we showed that the BCCAS model, which has been used as an experimental model of chronic hypoperfusion is firstly characterized by an acute and severe hypoperfusion leading to the rapid vascular response and ischemic lesions particularly affecting subcortical and watershed areas (striatum, corpus callosum and prefrontal cortex). The acute hemodynamic compensatory response leads to a gradual recovery and in the long-term a modest hypoperfusion. Therefore, BCCAS mice significantly differ from patients, where chronic hypoperfusion is a gradual phenomenon, occurring in years or decades and leaving the time for a progressive adaptation of collateral circulation both at the level of the circle of Willis and leptomeningeal collaterals. The compensatory responses triggered during this acute and most severely hypoperfused phase (1 day) are the main determinants of the long-term outcome both in terms of lesion volume, extension, recovery and brain atrophy. Thus, the loss of neurons reported in corpus callosum in the chronic phase in this BCCAS model²⁸ may be attributable to ischemic lesions and acute severe drop in CBF, rather than resulting from chronic mild global hypoperfusion.

In summary, we show that focal ischemia triggers a global hemodynamic response, significantly affecting also the contralateral hemisphere until the effective re-establishment of a new hemodynamic balance. Acute hypoperfusion immediately leads to a negative selection

of mice with no PcomAs. PcomA patency ipsilateral to the focal ischemia determines the infarct volume and recovery in MCAO mice. Similarly, the rapidity of retrograde ECA blood flow recruitment, together with PcomA patency, mainly shapes the extension and the side of ischemic lesions in BCCAS mice. Finally, given the significant intrastrain collateral variability, when using C57BL/6J mice as MCAO and BCCAS ischemia models to test the independent effect of neuroprotectants and genes on stroke outcome, PcomAs and the overall collateral recruitment particularly during the most severe brain hypoperfusion (one to seven days post-surgery) have to be critically considered as additive and main factors influencing brain lesions and perfusion recovery.

Acknowledgements

NeuroCure, Deutsches Zentrum für Neurodegenerative Erkrankungen (DZNE), Alexander von Humboldt Fellowship (to Celeste Sassi).

Authors' contributions

CS, MF, KW and UD and planned the experiments. CS, MF and KW performed the experiments. CS, MF, KW, UD, KB, SM, SB, NR, SCG, DH, AI, AM, AJ, OS, DB took part to the result analysis and manuscript revision.

Funding


The author(s) received no financial support for the research, authorship, and/or publication of this article.

Declaration of conflicting interests

The author(s) declared no potential conflicts of interest with respect to the research, authorship, and/or publication of this article.

ORCID iDs

Sonja Blumenau  <http://orcid.org/0000-0002-6606-3800>

Sergio Crespo-Garcia  <http://orcid.org/0000-0002-8640-9135>

Supplementary material

Supplementary material for this paper can be found at the journal website: <http://journals.sagepub.com/home/jcb>

References

1. Shuaib A, Butcher K, Mohammad AA, et al. Collateral blood vessels in acute ischaemic stroke: a potential therapeutic target. *Lancet Neurol* 2011; 10: 909–921.
2. Faber JE, Moore SM, Lucitti JL, et al. Sex differences in the cerebral collateral circulation. *Transl Stroke Res* 2017; 8: 273–283.
3. McColl BW, Carswell HV, McCulloch J, et al. Extension of cerebral hypoperfusion and ischaemic pathology

- beyond MCA territory after intraluminal filament occlusion in C57Bl/6J mice. *Brain Res* 2004; 997: 15–23.
4. Wang S, Zhang H, Dai X, et al. Genetic architecture underlying variation in extent and remodeling of the collateral circulation. *Circ Res* 2010; 107: 558–568.
 5. Chalothorn D, Clayton JA, Zhang H, et al. Collateral density, remodeling, and VEGF-A expression differ widely between mouse strains. *Physiol Genomics* 2007; 30: 179–191.
 6. Lucitti JL, Sealock R, Buckley BK, et al. Variants of Rab GTPase-effector binding protein-2 cause variation in the collateral circulation and severity of stroke. *Stroke* 2016; 47: 3022–3031.
 7. Boehm-Sturm P, Füchte-meier M, Foddis M, et al. Neuroimaging biomarkers predict brain structural connectivity change in a mouse model of vascular cognitive impairment. *Stroke* 2017; 48: 468–475.
 8. Martin NA, Bonner H, Elkjær ML, D’Orsi B, Chen G, König HG, et al. BID Mediates Oxygen-Glucose Deprivation-Induced Neuronal Injury in Organotypic Hippocampal Slice Cultures and Modulates Tissue Inflammation in a Transient Focal Cerebral Ischemia Model without Changing Lesion Volume. *Front Cell Neurosci* 2016; 10: 14.
 9. Zudaire E, Gambardella L, Kurcz C, et al. A computational tool for quantitative analysis of vascular networks. *PLoS ONE* 2011; 6: e27385.
 10. Kerty E, Nyberg-Hansen R, Hørven I, et al. Doppler study of the ophthalmic artery in patients with carotid occlusive disease. *Acta Neurol Scand* 1995; 92: 173–177.
 11. Kerty E, Eide N and Hørven I. Ocular hemodynamic changes in patients with high-grade carotid occlusive disease and development of chronic ocular ischaemia. II. Clinical findings. *Acta Ophthalmol Scand* 1995; 73: 72–76.
 12. Lagrèze HL, Levine RL, Pedula KL, et al. Contralateral flow reduction in unilateral stroke: evidence for transhemispheric diaschisis. *Stroke* 1987; 18: 882–886.
 13. Lavy S, Melamed E and Portnoy Z. The effect of cerebral infarction on the regional cerebral blood flow of the contralateral hemisphere. *Stroke* 1975; 6: 160–163.
 14. Takatsuru Y, Eto K, Kaneko R, et al. Critical role of the astrocyte for functional remodeling in contralateral hemisphere of somatosensory cortex after stroke. *J Neurosci* 2013; 33: 4683–4692.
 15. Krakauer JW, Radoeva PD, Zarahn E, et al. Hypoperfusion without stroke alters motor activation in the opposite hemisphere. *Ann Neurol* 2004; 56: 796–802.
 16. Sbarbati A, Reggiani A, Nicolato E, et al. Regional changes in the contralateral ‘healthy’ hemisphere after ischemic lesions evaluated by quantitative T2 parametric maps. *Anat Rec* 2002; 266: 118–122.
 17. Carmeliet P. Blood vessels and nerves: common signals, pathways and diseases. *Nat Rev Genet* 2003; 4: 710–720.
 18. Baron JC, Rougemont D, Soussaline F, et al. Local interrelationships of cerebral oxygen consumption and glucose utilization in normal subjects and in ischemic stroke patients: a positron tomography study. *J Cereb Blood Flow Metab* 1984; 4: 140–149.
 19. Xu C, Schmidt WUH, Galinovic I, et al. The potential of microvessel density in prediction of infarct growth: a two-month experimental study in vessel size imaging. *Cerebrovasc Dis* 2012; 33: 303–309.
 20. Kawabori M, Kacimi R, Kauppinen T, et al. Triggering receptor expressed on myeloid cells 2 (TREM2) deficiency attenuates phagocytic activities of microglia and exacerbates ischemic damage in experimental stroke. *J Neurosci* 2015; 35: 3384–3396.
 21. Jin W-N, Shi SX-Y, Li Z, et al. Depletion of microglia exacerbates postischemic inflammation and brain injury. *J Cereb Blood Flow Metab* 2017; 37: 2224–2236.
 22. Shimada K, Furukawa H, Wada K, et al. Protective role of peroxisome proliferator-activated receptor- γ in the development of intracranial aneurysm rupture. *Stroke* 2015; 46: 1664–1672.
 23. Silva RAP, Kung DK, Mitchell IJ, et al. Angiotensin 1–7 reduces mortality and rupture of intracranial aneurysms in mice. *Hypertension* 2014; 64: 362–368.
 24. Wiener J, Spiro D and Lattes RG. The cellular pathology of experimental hypertension. II. Arteriolar hyalinosis and fibrinoid change. *Am J Pathol* 1965; 47: 457–485.
 25. Greenberg SM, Vernooij MW, Cordonnier C, et al. Cerebral microbleeds: a guide to detection and interpretation. *Lancet Neurol* 2009; 8: 165–174.
 26. Gould DB, Phalan FC, van Mil SE, et al. Role of COL4A1 in small-vessel disease and hemorrhagic stroke. *N Engl J Med* 2006; 354: 1489–1496.
 27. Weng Y-C, Sonni A, Labelle-Dumais C, et al. COL4A1 mutations in patients with sporadic late-onset intracerebral hemorrhage. *Ann Neurol* 2012; 71: 470–477.
 28. Shibata M, Ohtani R, Ihara M, et al. White matter lesions and glial activation in a novel mouse model of chronic cerebral hypoperfusion. *Stroke* 2004; 35: 2598–2603.